

Frequency Control Analysis based on Unit Commitment Schemes with High Wind Power Integration: a Spanish Isolated Power System Case Study

Ana Fernández-Guillamón^a, José Ignacio Sarasúa^b, Manuel Chazarra^b, Antonio Viguera-Rodríguez^c, Daniel Fernández-Muñoz^b, Ángel Molina-García^{a,*}

^aDept. of Electrical Engineering, Universidad Politécnica de Cartagena, 30202 Cartagena, Spain

^bDept. of Hydraulic, Energy and Environmental Engineering, Universidad Politécnica de Madrid, 28040, Spain

^cDept. of Civil Engineering, Universidad Politécnica de Cartagena, 30202 Cartagena, Spain

Abstract

The relevant integration of wind power into the grid has involved a remarkable impact on power system operation, mainly in terms of security and reliability due to the inherent loss of the rotational inertia as a consequence of such new generation units decoupled from the grid. In these weak scenarios, the contribution of wind turbines to frequency control is considered as a suitable solution to improve system stability. With regard to frequency response analysis and grid stability, most contributions introduce wind control discuss generation tripping for isolated power systems under arbitrary power imbalance conditions. Frequency response is then analyzed for hypothetical imbalances usually ranged between 5% and 20%, and assuming averaged energy schedule scenarios. In this paper, a more realistic framework is proposed to evaluate frequency deviations by including high wind power integration. With this aim, unit commitment schemes and frequency load shedding are considered in this work for frequency response analysis under high wind power penetration. The Gran Canaria Island's isolated power system (Spain) is used for evaluation purposes. Results provide a variety of influences from wind frequency control depending not only on the wind power integration, but also the generation units under operation, the rotational inertia reductions as well as the available reserves from each resource, aspects that have not been addressed previously in the specific literature to evaluate frequency excursions under high wind power integration.

Keywords: Power system stability, Wind energy integration, Wind frequency control, Unit commitment

Nomenclature

cc	Combined cycle (subscript)
ds	Diesel (subscript)
D	Load-frequency sensitivity parameter (damping factor)
f	Frequency
g	Gas (subscript)
K	Participation factor
H_i	Rotational inertia of synchronous generator i
h_{WT}	Number of wind turbines
P_i	Power supplied by generation units i
P_d	Power demand
P_J	Power of <i>Jinámar</i> power plant
P_{MPPT}	Maximum power point of wind turbines
P_{sp}	Set-point active power of wind turbines
P_T	Power of <i>Barranco de Tirijana</i> power plant
P_w	Power of wind power plants
RR	Regulation effort

s	Steam (subscript)
$T_m(t)$	Inertia of the power system
$T_{u,th}$	Secondary response time constant
v_w	Wind speed
AGC	Automatic generation control
RES	Renewable energy sources
MILP	Mixed integer linear programming
RoCoF	Rate of change of frequency
TSO	Transmission system operator
UC	Unit commitment
VSWT	Variable speed wind turbines

1. Introduction

Conventional power plants with synchronous generators have traditionally determined the inertia of power systems [1]. However, during the last decades, most countries have promoted large-scale integration of Renewable Energy Sources (RES) [2, 3]. RES are usually not connected to the grid through synchronous machines, but through power electronic converters electrically decoupled from the grid [4, 5]. As a consequence, by increasing the amount of RES and replacing synchronous conventional units, the effective rotational inertia of power systems can be significantly reduced [6–8]. Actually, Albadi *et al.* consider

*Corresponding author

Email addresses: ana.fernandez@upct.es (Ana Fernández-Guillamón), joseignacio.sarasua@upm.es (José Ignacio Sarasúa), manuel.chazarra@upm.es (Manuel Chazarra), aviguera.rodriguez@upct.es (Antonio Viguera-Rodríguez), daniel.fernandezm@upm.es (Daniel Fernández-Muñoz), angel.molina@upct.es (Ángel Molina-García)

that the impact of RES on power systems mainly depends on the RES integration and the system inertia [9], being the RES negative effects more severe in isolated power systems [10]. Among the different RES, wind power is the most developed and relatively mature technology [11], especially variable speed wind turbines (VSWT) [12–16]. Indeed, Toulabi *et al.* affirm that the participation of wind power into frequency control services becomes inevitable due to the relevant integration of such resource [17].

Power imbalances between generation and demand can occur, among others, due to the loss of power generators [18]. Actually, this loss of power generators can be the most severe contingency in case it is the largest one [19]. These imbalances cause frequency fluctuations, and subsequently the grid becomes unstable, even leading to blackouts [20, 21]. Hence, the frequency control services are playing an essential role for secure and reliable power systems [22]. Moreover, frequency stability is the most critical issue in isolated power systems due to their low rotational inertia [23–25]. Frequency control has a hierarchical structure, and in Europe is usually organized up to five layers: (i) frequency containment, (ii) imbalance netting, (iii, iv) frequency restoration (automatic and/or manual) and (v) replacement, from fast to slow timescales [26].

According to the specific literature, several studies have proposed wind frequency control approaches. However, authors notice that in those contributions: (i) energy schedule scenarios considered are usually arbitrary and unrealistic, without considering a unit commitment (UC) scheme and individual generation units [27–31]; (ii) the power imbalance is usually taken as a fixed random value (between 3 and 20%), excluding the $N - 1$ criterion [32–35]; (iii) load shedding is not taken into account in the frequency response analysis [36–38]; and (iv) only a few wind power integration scenarios are commonly analyzed to evaluate the wind frequency controller —usually one or two different scenarios— [39–42]. As a consequence, simulations can address unrealistic and inaccurate results. For instance, recent studies considering two wind integration share rates provide different —and even opposite— conclusions regarding frequency nadir and RoCoF (Rate of Change of Frequency): some authors conclude that these parameters can improve [33, 43], others that they could get worse [31, 44] or even be similar [34] as wind penetration increases.

By considering previous contributions, the aim of this paper is to analyze the frequency response of an isolated power system with high integration of wind power generation including wind frequency control and load shedding. These energy schedule scenarios are determined by a UC model, taking into account some technical and economical constraints [45] and guaranteeing the frequency system recovery after the largest power plant outage ($N - 1$ criterion) [46]. A realistic load shedding program is also included, as well as wind frequency control. With this aim, our study is carried out in Gran Canaria Island power system, in the Canary island archipelago (Spain), where the

wind power integration has increased from 90 to 180 MW in the last two years. Moreover, in the Canary island archipelago, more than 200 loss of generation events per year were registered between 2005 and 2010. In fact, the number of this kind of incidents even surpassed 300 per year, subsequently suffering from the activation of the load shedding programs [47]. This analysis can be extended to other isolated power systems with relevant wind energy potential, such as Madagascar [48] or Japan [49]. The main contributions of this paper can be thus summarized as follows:

- Evaluation of wind frequency control responses, including load shedding and rotational inertia changes from realistic operation conditions under generation unit tripping.
- Analysis of frequency deviations (nadir, RoCoF) in isolated power systems with high penetration of wind power, using energy schedules and unit comments obtained from an optimization model.

The rest of the paper is organized as follows: Section 2 describes the Gran Canaria power system and the generation scheduling process. The power system model, including both optimization and dynamic models, are described in Section 3. Simulation results are analyzed and discussed in Section 4. Finally, Section 5 outlines the main conclusions of the paper.

2. Power System and Generation Scheduling Process

2.1. Preliminaries

Different frequency analysis studies have been carried out by authors based on specific power systems. For instance, Zerket *et al.* considered a modified Nordic 32-bus test system [50]; in [51], the power system of Flores Island, and the electric power system of Sao Miguel Island were used; Moghadam *et al.* focused on the power system of Ireland [52]; in [53], the Singapore power system was used; Pradhan *et al.* tested the three-area New England system [54]; and [55] considered the Spanish isolated power system located in El Hierro Island. In this paper, authors have focused on Gran Canaria Island (Spain), where the wind power integration has increased from 90 to 180 MW in the last two years.

Gran Canaria Island belongs to Canarian archipelago, one of the outermost regions of the European Union. Canarian archipelago is located in the north-west of the African Continent. From the energy point of view, Gran Canaria Island is an isolated power system. Traditionally, Gran Canaria Island’s generation has been exclusively associated with fossil fuels: diesel, steam, gas and combined cycle units from two different power plants: *Jinámar power plant* and *Barranco de Tirijana power plant*. However, this fossil fuel dependence has involved an important economic and environmental drawback. To overcome these

problems, the Canary Government promoted the installation of wind power plants in the 90's, accounting for 70 MW in 2002. In the following decade, the installation of wind power plants stopped around 95 MW and, since 2015, wind power capacity has been doubled, nearly reaching 180 MW.

Regarding the wind power generation and system demand in Gran Canaria Island along 2018, both are shown in Fig. 1. The system demand is discretized for six different intervals, considering the lowest and highest demand of Gran Canaria Island. Wind power generation is discretized for five intervals. According to the ranges in the system demand and the wind power generation shown in Fig. 1, thirty energy scenarios are proposed to analyse the frequency response of the system including wind frequency control. Each energy scenario is based on a pair demand-wind power generation as it is further described in Section 4.

2.2. Generation Scheduling Process

The generation scheduling of the Gran Canaria Island power system is ruled in [57, 58]. It is carried out by the Spanish Transmission System Operator (TSO) according to the economic criterion of variable costs of each power plant. The schedules are obtained according to different time horizons: weekly or daily. Each energy schedule depends on the previous time horizon and, subsequently, weekly and daily schedules are required to determine the hourly generation scheduling, which is used in the present paper. An overview of these schedules is summarized in Fig. 2.

1. *Weekly scheduling*: Estimation of the hourly start-up and shut-down decisions from each Saturday (00:00 h) to the following Friday (23:59 h). This initial generation schedule is determined following two steps: (i) an economic dispatch is carried out to minimize the total variable costs to meet the net power system demand (i.e., the power system demand minus the renewable generation). The result of such economic dispatch includes both the hourly energy and the reserve schedules (labeled as **Schedule-A**). (ii) an economic and security dispatch is determined taking into account the transmission lines and minimizing the total variable costs to support the net power system demand and a certain level of power quality. The result of this economic and security dispatch is also a hourly energy and reserve schedule (labeled as **Schedule-B**).
2. *Daily scheduling*: Updates the **Schedule-B** of a certain day D from the updated available information of the power system: generation from suppliers, demand from consumers and the state of the transmission lines. The result of the daily scheduling in the day D is a new hourly energy and reserve schedule (labeled as **Schedule-C**). It is obtained before 14:00 h of the day $D - 1$. This **Schedule-C** is determined

following a similar process as in the weekly scheduling: (i) an economic dispatch is firstly carried out and (ii) an economic and security dispatch is then calculated. The daily scheduling processes aims to minimize the total variable costs to meet the net power system demand with a minimum certain level of power quality.

3. Methodology: Unit Commitment and Frequency Model

Frequency deviations are analyzed according to possible generation tripping and power system reserves by considering explicitly individual generation units and technologies. With this aim, a series of energy scenarios for each scenario of system demand and wind power generation based on a real isolated power system (the Gran Canaria Island) are estimated and evaluated accordingly, considering current wind power integration percentages and load shedding programs. Fig. 3 shows the proposed methodology, highlighting the novelties and differences presented in this paper compared to other approaches focused on frequency analysis (i.e., carry out a UC to determine the energy scenarios, consider the loss of the largest power plant as imbalance, and include load shedding with and without wind frequency control). The following subsections describe respectively the unit commitment model and frequency models used in this work. Fig. 4 shows a simplified scheme of the modelled Gran Canaria Island power system, where conventional and wind power plants are depicted.

3.1. Unit commitment model: creation of scenarios

In order to analyze frequency deviations in the Gran Canaria power system, a UC model is required to estimate the number of thermal units connected to the grid for each generation mix scenario. These thermal units remain unchanged during the subsequent frequency control analysis. The UC model used in this paper has been recently proposed by the authors in [59], based on [60], which is a deterministic thermal model based on mixed integer linear programming (MILP). Other contributions focused on probabilistic unit commitment can be also found in the specific literature. In this way, [61] proposes an optimal allocation of up/down spinning reserves under high integration of wind power. The planning horizon of our model is adapted to 24 hours with a time resolution of one hour consistent with the approach used by the TSO for the next-day generation scheduling [62]; and the hydropower technology is excluded from the model formulation in order to be consistent with the generation mix of the Gran Canaria power system. The model formulation is partially based on [63] which is, to the author's knowledge, the most computationally efficient formulation available in the literature when considering different types of start-up costs of thermal units.

The Gran Canaria power system is operated in a centralized manner by the TSO in order to minimize the total

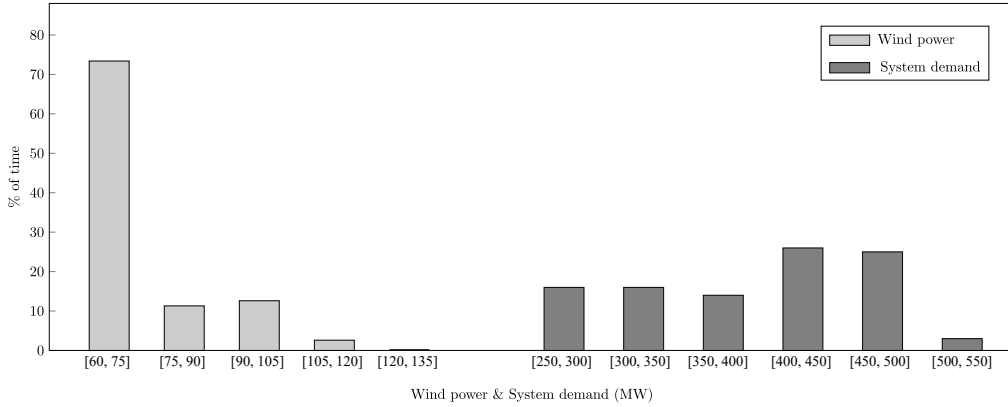


Figure 1: Wind power generation and system demand distribution in Gran Canaria Island power system along 2018 [56].

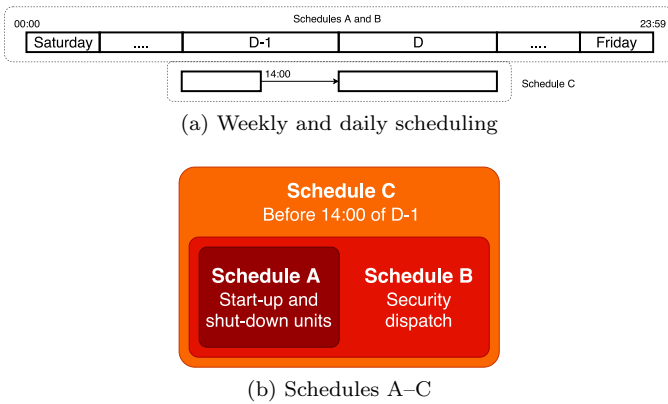


Figure 2: Generation scheduling of Gran Canaria Island power system

system costs, according to [58]. Therefore, the objective function of the UC model here used consists in minimizing the start-up cost, the fuel cost, the operation and maintenance cost and the wear and tear cost of all thermal units. The optimal solution of the UC model is formed by the hourly energy schedule of each thermal unit of the system, taking into account their minimum on-line and off-line times. Among others, the energy schedule is restricted by the following constraints. The production-cost curve of each thermal unit is modeled as a piece-wise linear function discretized by ten pieces. The number of pieces is determined as a trade-off between the accuracy of the solution and the computation time cost limits. In addition, the system demand and the spinning reserve requirements must be fulfilled in each hour. According to the P.O. SEIE 1 in [57], the hourly spinning reserve must be higher or equal to the maximum of the following three values: (i) the expected inter-hourly increase in the system demand between two consecutive hours; (ii) the most likely wind power loss calculated by the TSO from historical data; (iii) the loss of the largest spinning generating unit in each hour. It is important to bear in mind that there are two conceptual differences between the formulation presented in [63] and the one used here:

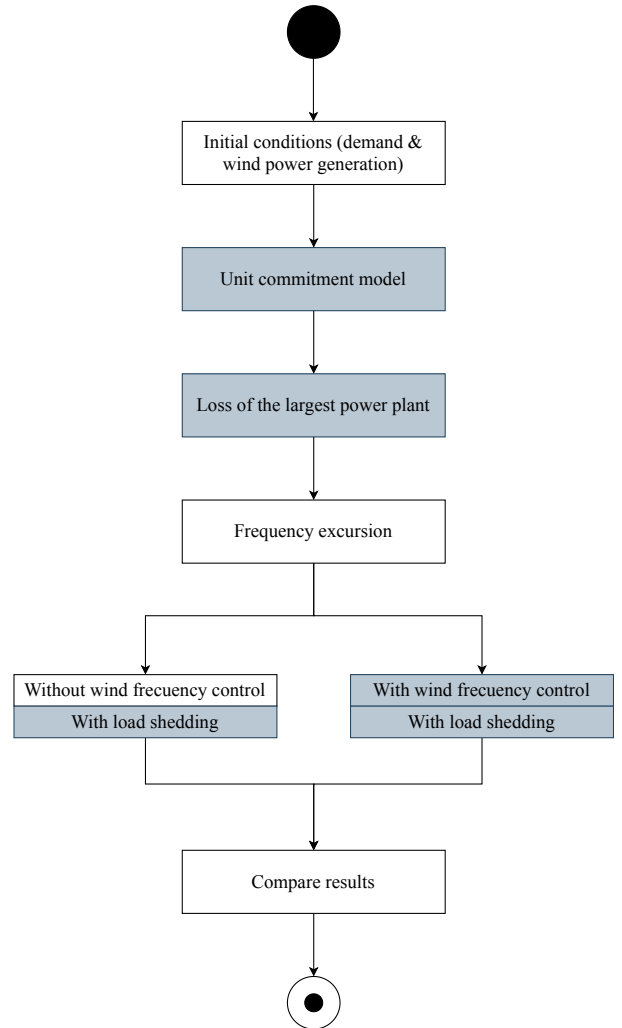


Figure 3: Flow chart of the methodology used

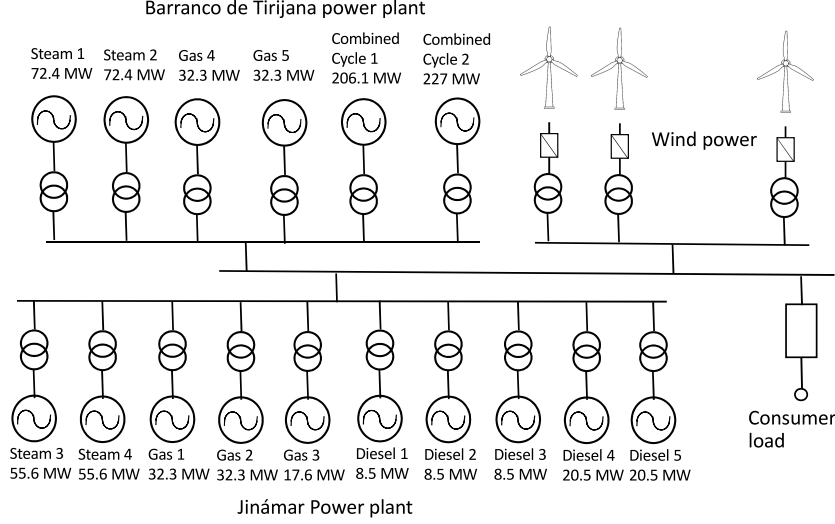


Figure 4: Gran Canaria Island power system, simplified one-line diagram

- The meaning of each start-up type of each thermal unit is different. In [63], each start-up type corresponds to a different power trajectory of the thermal unit whereas the approach of the model here used is the following: each start-up type refers to the start-up cost as a function of the time that the unit has remained off-line since the previous shut-down. The start-up cost calculation and the involved parameters of the thermal units are defined in [58].
- For those thermal units that have a start-up process longer than one hour, a single output power trajectory ranging from zero to the unit's minimum output power is considered.

Further details of the UC model formulation can be found in [59].

3.2. Frequency analysis model

3.2.1. General overview

Frequency deviations in power systems are usually modeled by means of an aggregated inertial model. This assumption has been successfully applied to isolated power systems, as the Irish power system [64]. In this paper, frequency system variations are the result of an imbalance between the supply-side (*Barranco de Tirijana* power plant P_T , *Jinámar* power plant P_J and wind power plants P_w , which are explicitly considered for simulations) and the demand-side P_d . A load frequency sensitivity parameter D is also included to model the load sensitivity under frequency excursions [65],

$$f \frac{df}{dt} = \frac{1}{T_m(t)} (P_T + P_J + P_w - P_d - D \cdot \Delta f), \quad (1)$$

being $T_m(t)$ the total inertia of the power system, which corresponds to the equivalent addition of the rotational

inertia of all synchronous generators under operation conditions, in terms of the system base,

$$T_m(t) = \sum_{m=1}^4 2 H_{s,m} + \sum_{q=1}^5 2 H_{g,q} + \sum_{k=1}^5 2 H_{ds,k} + \sum_{l=1}^2 2 H_{cc,l}. \quad (2)$$

Frequency and power variables also depend on time, but it is not explicitly included to simplify the expressions. Fig. 5 shows the general block diagram of the proposed simulation model. It has been developed in Matlab/Simulink. The block 'Power system' in Fig. 5 contains eq. (1), modeled with the corresponding block diagram. The power provided by the power plants, P_T and P_J respectively, are the addition of the power supplied by each thermal generation unit (steam s , gas g , combined cycle cc and diesel ds) under operating conditions, expressed as follows:

$$P_T = \sum_{m=1}^2 P_{s,m} + \sum_{q=4}^5 P_{g,q} + \sum_{l=1}^2 P_{cc,l}, \quad (3)$$

$$P_J = \sum_{m=3}^4 P_{s,m} + \sum_{q=1}^3 P_{g,i} + \sum_{k=1}^5 P_{ds,k}. \quad (4)$$

The k , l , m and q indexes refer to the number of diesel, combined cycle, steam and gas units of each power plant, respectively. The proposed dynamic model depicted in Fig. 5 is thus composed by the different thermal units belonging to *Barranco de Tirijana* and *Jinámar* power plants—explicitly considered in the model—, as well as the wind power plants, the power system and the power load of consumers. This load consumer block includes the load shedding program, activated when the grid frequency exceed certain thresholds. The dynamic response of each generation unit is simulated according to the transfer functions discussed in Section 3.2.2.

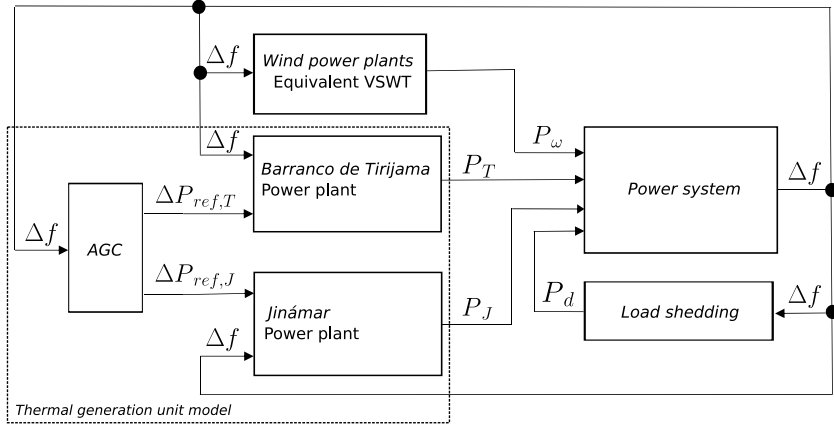


Figure 5: Frequency analysis model. Block diagram.

Table 1: Block diagram parameters of thermal units models [66, 67]

Gas and combined cycle units		Diesel units		Steam units	
TR_g	0.05 s	$T1_d$	0.01 s	TR_s	0.2 s
$T1_g$	0.6 s	$T2_d$	0.0 s	TSM_s	0.1 s
$T2_g$	0.5 s	$T3_d$	2.0 s	TCH_s	0.3 s
$T3_g$	0.01 s	$T4_d$	0.1 s	R_s	0.05 pu
$T4_g$	0.24 s	$T5_d$	0.1 s	H_s	5 s
TD_g	0.2 s	$T6_d$	0.1 s		
R_g	0.05 pu	K_d	3		
R_{cc}	0.05 pu	R_d	0.05 pu		
H_g	5 s	H_d	2.45 s		
H_{cc}	5 s				

Table 2: Load shedding scheme.

Step	Threshold (Hz)	Delay (s)	Load shedding (MW)	
			Peak demand	Valley demand
1	48.9	0.1	14.6	5.8
2	48.9	0.2	16.2	7.0
3	48.8	0.4	17.1	8.6
4	48.8	0.6	41.1	18.8
5	48.5	0.1	8.0	4.1
6	48.5	0.2	27.3	11.8
7	48.4	0.4	17.5	7.7
8	48.1	0.1	17.9	9.7

3.2.2. Thermal generation units

The frequency response of the thermal generation units has been modeled through the transfer functions proposed in [66, 67]. Parameters have been selected from typical values, see Table 1. The combined cycle generation unit frequency behavior is supposed similar to the gas generation units, see Fig. 6. The two inputs for these three frequency models are (i) frequency deviations—including constraints provided by the frequency containment—and, (ii) AGC conditions for the frequency restoration in isolated power systems. Both inputs are linked by the corresponding droop.

According to the Spanish insular power system requirements, the AGC system is in charge of removing the steady-state frequency error after the frequency containment control. This is usually known as ‘frequency restoration’, and modeled in a similar way to [68]. The equivalent regulation effort ΔRR is then estimated as:

$$\Delta RR = -K_f \cdot \Delta f. \quad (5)$$

This expression is included in the block diagram shown Fig. 5, in block ‘AGC’. K_f is determined following the ENTSO-E recommendations [69]. This regulation effort is conducted by all thermal generation units and distributed depending on the participation factors $K_{u,i}$, assuming that: (i) all thermal generation units connected to the power system equally participate in secondary regulation control and (ii) the participation factors are obtained as

a function of the speed droop of each unit. The participation factors $K_{u,i}$ of thermal generation units disconnected from the grid are considered as zero [70]:

$$\begin{aligned} \Delta P_{ref,th} &= \frac{1}{T_{u,th}} \int \Delta RR \cdot K_{u,th} dt = \\ &= \frac{-1}{T_{u,th}} \cdot K_{u,th} \cdot K_f \int \Delta f dt. \end{aligned} \quad (6)$$

$$\begin{aligned} \sum K_{u,th} &= \sum_{m=1}^4 K_{u,s,m} + \sum_{q=1}^5 K_{u,g,q} + \\ &+ \sum_{k=1}^5 K_{u,d,k} + \sum_{l=1}^2 K_{u,cc,l} = 1 \end{aligned} \quad (7)$$

3.2.3. Load shedding

A realistic load shedding scheme is considered in the proposed model by means of sudden load disconnections when frequency excursions are higher than certain thresholds. Table 2 summarizes these frequency thresholds, time delay and load shedding values for different scenarios. This load shedding scheme depends on the islanding power system operation conditions required by the Spanish TSO and thus, the responses are in line with certain frequency excursion thresholds. When the scenario corresponds to an intermediate load case, the load shedding value is interpolated from the corresponding steps.

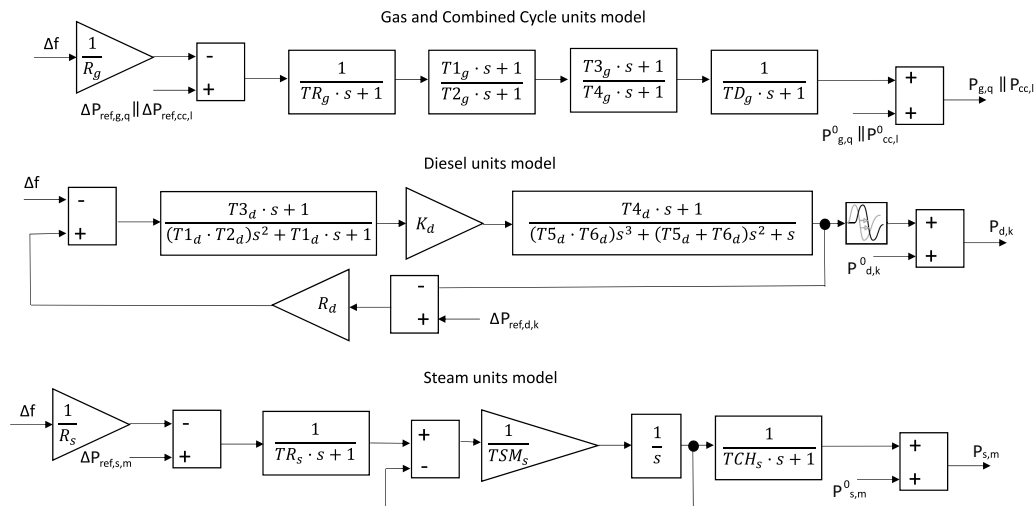


Figure 6: Block diagrams of thermal units models.

3.2.4. Wind power plants

One equivalent VSWT with n_{WT} -times the size of each one model the wind power penetration —being n_{WT} the number of wind turbines [71, 72]—, is proposed as aggregated model for wind power plants. An equivalent averaged wind speed ($v_w = 10.25$ m/s) is assumed for the simulations. This wind speed is considered as constant, which has been previously used in the specific literature for short-time period frequency analysis including wind power plants [50, 73–76]. With this wind speed, the wind generation accounts for 80% of the installed wind power capacity.

Wind turbines are modeled according to the turbine control model, mechanical two-mass model and wind power model described in [77, 78]. The two-mass model assumes the rotor and blades as a single mass, and the generator as another mass [79, 80]. Huerta *et al.* consider that the two-mass model is the most suitable to evaluate the grid stability [81]. Wind turbines also include a frequency control response. The strategy for VSWTs implemented in this paper is based on the technique described in [82, 83], see Fig. 7a. It was evaluated in [82] for isolated power systems with up to a 45% of wind power integration and compared to the approach of [84], providing a more appropriate frequency response under power imbalance conditions. In [83], the proposed frequency control strategy was studied for multi-area power systems. Three operation modes are considered: (i) normal operation mode, (ii) overproduction mode and (iii) recovery mode. Different set-point active power P_{sp} values are then determined aiming to restore the grid frequency under power imbalance conditions. Fig. 7b depicts the VSWTs active power variations ΔP_{WF} submitted to an under-frequency excursion, being $\Delta P_w = P_{sp} - P_{MPPT}(\Omega_{MPPT})$.

With the aim of reducing load shedding contributions under high wind power integration scenarios, two modifications are carried out to the preliminary frequency con-

troller, both in overproduction and recovery periods. According to [82], the overproduction power ΔP_{OP} is estimated proportionally to the frequency excursion evolution, with a maximum value of 10%. In this paper, the maximum ΔP_{OP} is increased to 15%, in order to provide more power after the imbalance and minimizing load shedding situations. In the recovery mode, the power of point P_2 is defined as $P_{MPPT}(\Omega_V) + x \cdot (P_{mt}(\Omega_V) - P_{MPPT}(\Omega_V))$ —see Fig. 7a—, being x a scale factor considered as 0.75 in the original approach [82]. However, in this case, the recovery time period of the wind turbines is faster than the AGC action of the frequency restoration control, and subsequently obtaining an undesirable frequency evolution, see Fig. 9. As a consequence, x has been increased to 0.95, smoothing and slowing down the recovery period of the wind frequency controller. This alternative frequency controller is included in the VSWT model as seen in Fig. 8.

4. Results

4.1. Scenarios under consideration

According to the demand distribution in Gran Canaria Island along 2018 previously discussed in Section 2.1, six different power demand conditions are considered for the study. Each system demand is analyzed under different wind power generation percentages following Fig. 1. Thus, thirty different energy scenarios are under study, which is significantly higher than other contributions focused on frequency control under contingencies including wind power plants [85, 86]. To determine the energy schedule of each supply-demand scenario, the Unit Commitment model described in Section 3.1 is run with GAMS software and Cplex 12.2 solver, which uses a branch and cut algorithm to solve MILP problems. Fig. 10 depicts the energy schedule of each scenario aggregated by generation technology. From the $N - 1$ criterion, the largest generation unit is suddenly disconnected under a contingency.

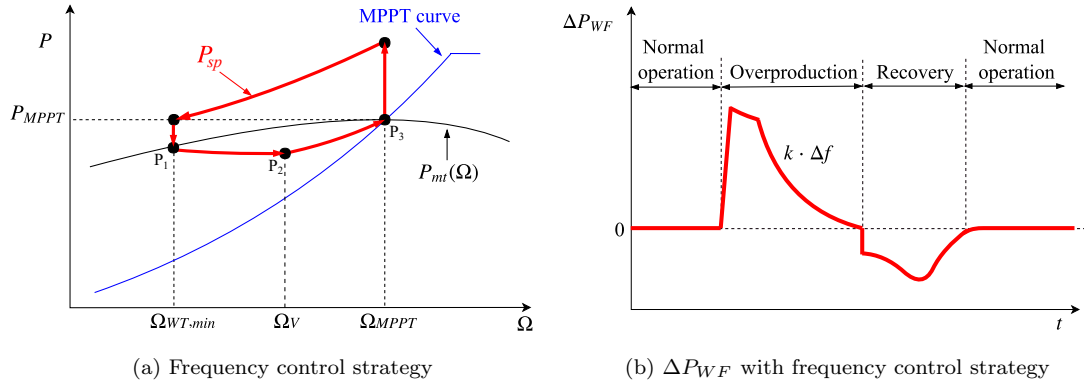


Figure 7: Wind frequency control strategy and VSWTs active power variation [82].

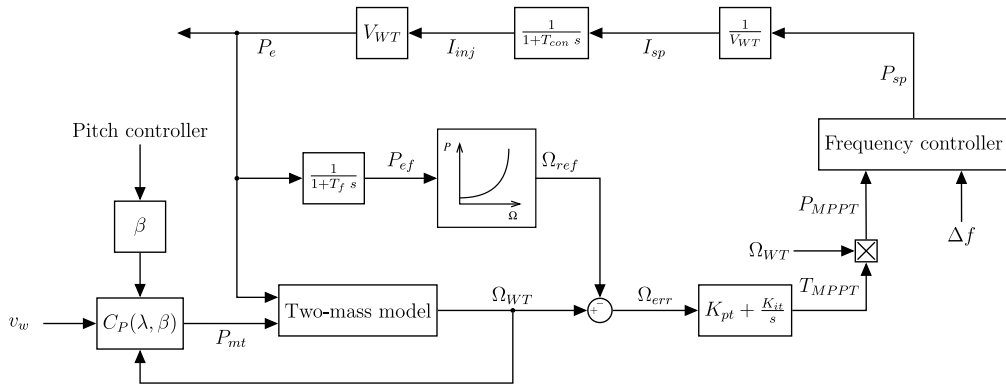


Figure 8: Variable speed wind turbine model with frequency controller

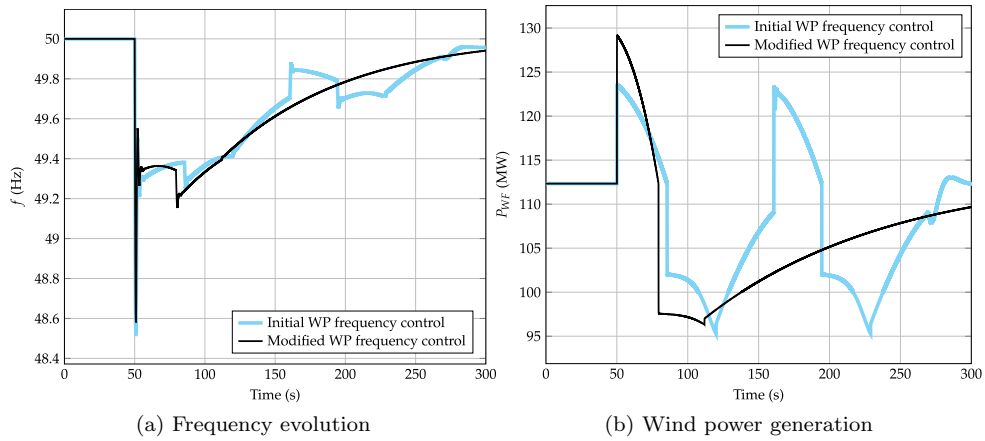


Figure 9: Frequency deviation and wind power generation when using the original wind frequency controller

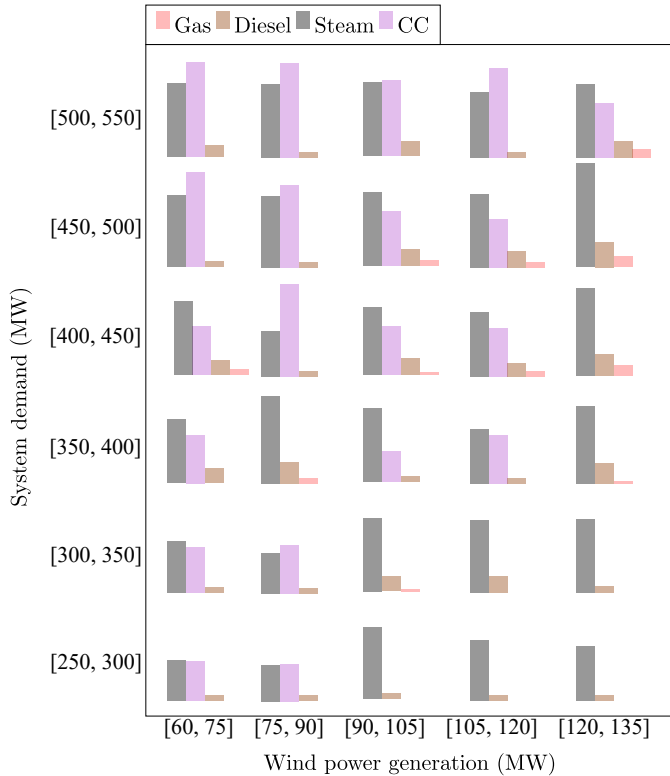


Figure 10: Scenarios under study

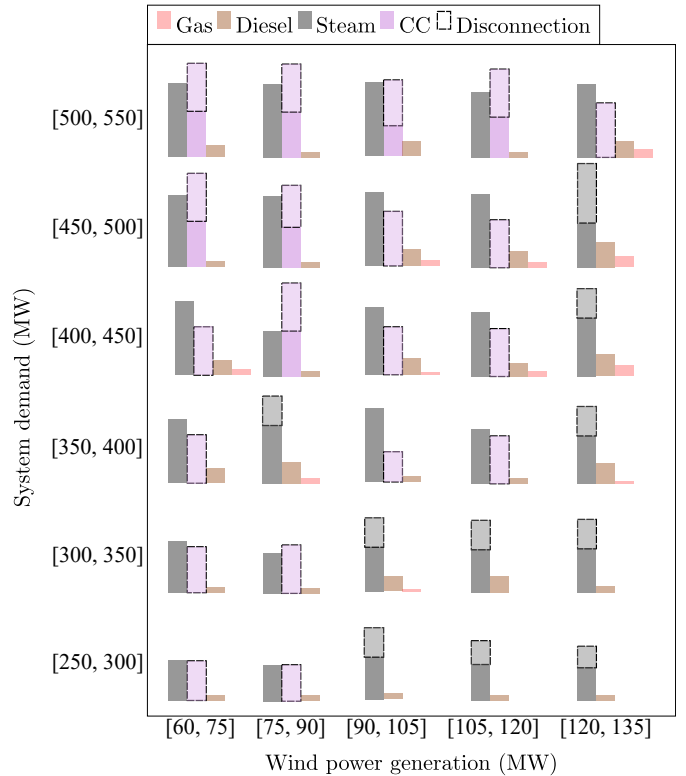


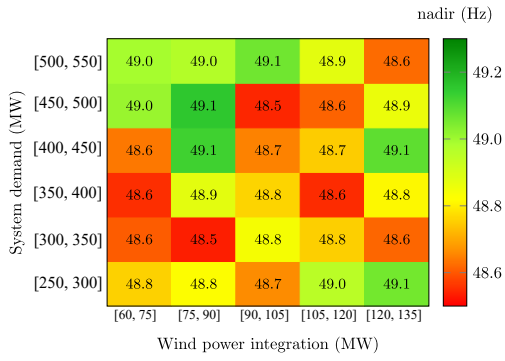
Figure 11: Generation mix after disconnections

As a consequence, a different generation group is disconnected in each scenario, depending on the energy schedule obtained by the UC model and subsequently addressed a variety of power imbalance situations. Fig. 11 summarizes the energy schedule of each scenario after these disconnections, pointed out the technology and generation unit tripping under such circumstances. Due to these sudden disconnections, the equivalent rotational inertia of the power system is reduced according to eq. (2).

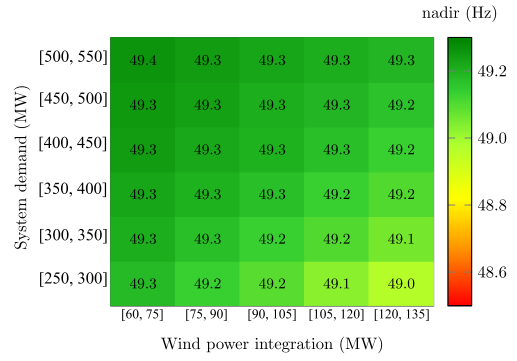
4.2. Frequency response analysis

With the aim of evaluating frequency deviation and power system performance under the sudden generation disconnection established with the $N-1$ criterion, grid frequency response is analyzed (*i*) excluding wind frequency control and only considering conventional units; and (*ii*) including conventional units and wind frequency control strategy. Firstly, nadir and RoCoF results for the 30 simulated scenarios according to the generation unit tripping obtained for the UC model and depicted in Fig. 11 are compared to results obtained following methodologies of previous contributions [27, 28, 31, 32]. They usually assume a constant 10% imbalance, neglect any inertia power system modification and do not include load shedding scheme in their frequency analysis models. With this aim, Figs 12 and 13 summarize nadir and RoCoF respectively, including (or not) wind frequency response. RoCoF is calculated between 0.3 and 0.5 s after the sudden disconnection of the largest conventional generation unit for each energy

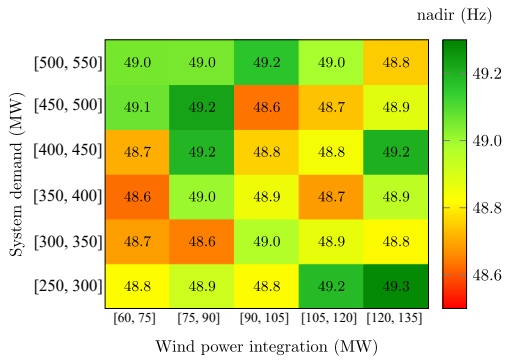
scenario. As can be seen, clear differences are identified between both approaches. In fact, most obvious results are determined with a constant power imbalance, as was to be expected, see Fig. 12b and 12d for nadir comparison values. If a simplified power system modeling is considered for frequency control analysis, with typical 10% power imbalance conditions—usually assumed in previous contributions as was previously discussed—49.4 Hz nadir and 0.5 Hz/s RoCoF values are obtained for all cases, which provides significant discrepancies with our proposal, see Fig. 12 and 13 respectively. Indeed, nadir lies in between 48.54 and 49.15 Hz when wind power plants are excluded from frequency control, depending on each scenario—see Fig. 12a—. In fact, these values were even worse if the load shedding program was not considered, as it is activated in 21 of the 30 scenarios analyzed. However, a larger wind power integration without frequency control—see Fig. 12a—doesn't imply a worse nadir response, which could be deduced a priori, due to the loss of the larger power plant (which is different, depending on the scenario). When wind frequency control is considered for simulations, the minimum frequency is increased 110 mHz in average for all cases. Moreover, the more wind power integration providing frequency control, the lower nadir is obtained. For instance, for wind power integration over 50%, the minimum frequency is reduced around 200 mHz. It can't be then deduced an homogeneous response of the considered power system submitted to realistic generation unit tripping. In this way, and based on the proposed



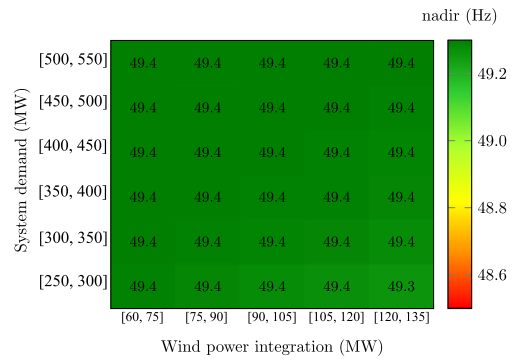
(a) Without wind frequency response



(b) Without wind frequency response and $\Delta P = 10\%$

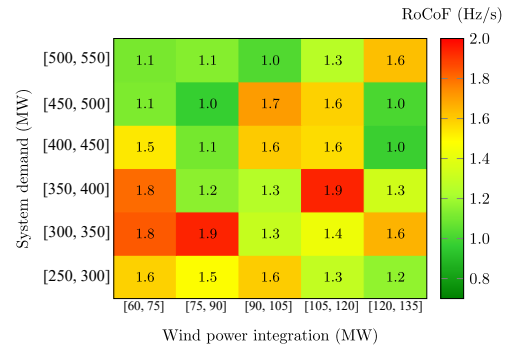


(c) With wind frequency response

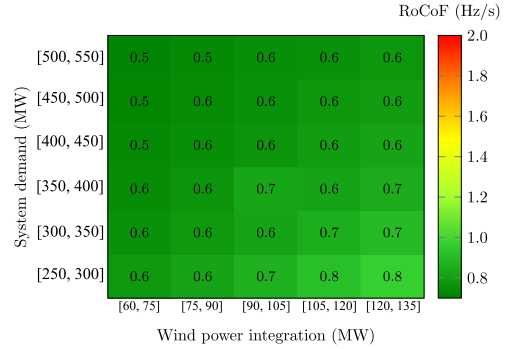


(d) With wind frequency response and $\Delta P = 10\%$

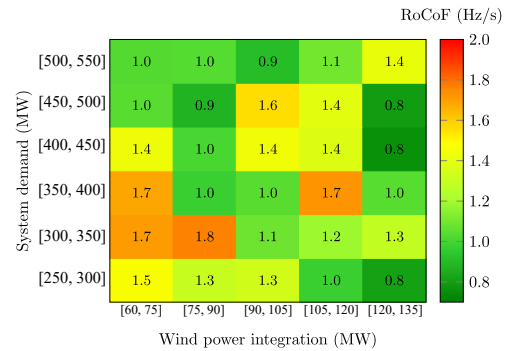
Figure 12: Nadir estimation: power demand and wind power integration in Gran Canaria



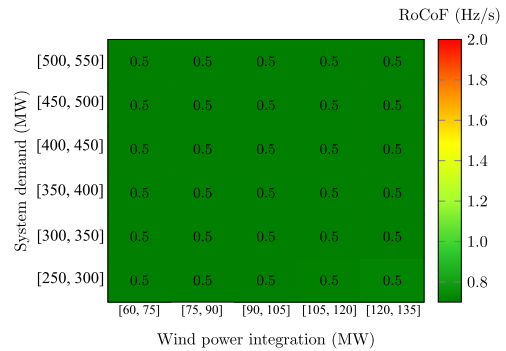
(a) Without wind frequency response



(b) Without wind frequency response and $\Delta P = 10\%$

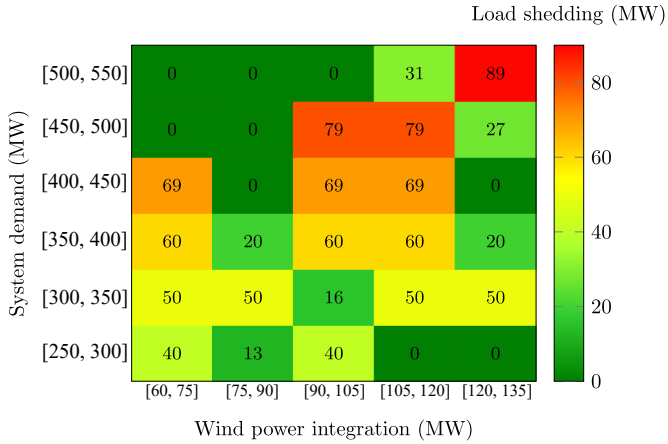


(c) With wind frequency response

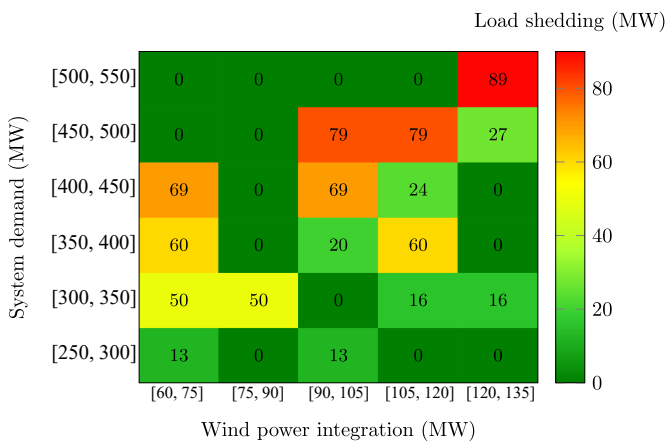


(d) With wind frequency response and $\Delta P = 10\%$

Figure 13: RoCoF estimation: power demand and wind power integration in Gran Canaria



(a) Load shedding without wind power frequency response



(b) Load shedding with wind power frequency response

Figure 14: Load shedding: power demand and wind power integration in Gran Canaria

methodology and modeling, it is important to point out that higher wind power integration excluding frequency control does not always imply a worse frequency response, see Fig. 12a. With regard to RoCoF, it varies between 0.97 and 1.93 Hz/s initially, see Fig. 13a, but slightly 185 mHz/s in average by including wind frequency control, Fig. 13c. These results are substantially different from those obtained in the simplified power system analysis (where RoCoF was around 0.5 Hz/s); this is mainly due to the inertia change considered in this study and neglected in the previous one, as low inertia is related to a faster ROCOF [87]. Therefore, including wind power frequency control can lead to lower frequency deviations under imbalances, as was expected.

The proposed wind frequency response analysis allows us to evaluate the wind frequency control impact on load shedding actions in islanding power systems under different imbalances. Fig. 14 summarizes the load shedding for the 30 simulated scenarios and considering the generation unit tripping obtained for the UC model, see Fig. 11. In this way, Fig. 14a and Fig. 14b shows the corresponding load shedding responses by including or not wind fre-

quency control for the considered energy scenarios. Both nadir and RoCoF improvements lead to a load shedding reduction in 11 scenarios. Moreover, in these 11 scenarios, the average load shedding reduction is 80%, getting up to a 100% reduction in 5 scenarios—for example, compare 30.80 MW load shedding under the range [500, 550] MW power demand and [105, 120] MW wind power generation, Fig. 14a, to 0 MW load shedding under the same demand and wind power values when wind frequency control is included, Fig. 14b—.

Table 3 shows a comparison of results between the proposed analysis described in this paper and conventional methodologies previously considered where a constant imbalance is assumed, inertia of the power system is kept constant during the imbalance and load shedding is not included for simulations. In the table, the average μ and variance σ^2 of nadir, RoCoF inertia change and load shedding values for the 30 different generation mix and imbalance scenarios are shown with and without wind frequency control.

5. Conclusion

Frequency excursions are analyzed in an isolated power system by considering the loss of the largest conventional generation group, including wind frequency control strategy, load shedding and energy scenarios obtained by a UC model. The case study is focused on the real isolated power system located in the Gran Canaria Island (Spain), which has doubled its wind power capacity in the last two years. With regard to the frequency analysis, by including wind power generation into frequency control, nadir and RoCoF are reduced in most of energy scenarios considered (110 mHz and 185 mHz/s in average, respectively). Regarding load shedding, it is reduced in 11 out of the 30 power imbalance analyzed. This improvement is more significant in high wind power integration scenarios (regardless of the power demand), and for high power demands (regardless of the wind power integration). Therefore, wind frequency control can be considered a remarkable solution to reduce load shedding in islanding power systems with high wind power integration.

It can be affirmed that there is no homogeneity in the frequency response results, providing a clear dependence on the dispatch of the conventional rotational generation units, their participation in the global energy scenario and the inertia changes addressed by the generation unit tripping—for example $\mu(\Delta f) = 1.2$ Hz and $\sigma^2(\Delta f) = 0.036$ for the nadir results. Subsequently, the participation of wind power plants into frequency control should be analyzed by considering not only the wind power integration level, but also other variables, such as the energy scenario, the rate power of the different generation units, as well as the reserves provided by conventional generation units and thus, the equivalent rotational inertia given by them; aspects that have not explicitly taken into account in previous works. Indeed, nadir and RoCoF values give almost

Table 3: Comparison of results: nadir, RoCoF, inertia change and load shedding

		Without wind frequency control		With wind frequency control	
		μ	σ^2	μ	σ^2
Proposed analysis	nadir (Hz)	48.8	0.036	48.9	0.037
	RoCoF (Hz/s)	1.4	0.085	1.2	0.085
	Inertia change (s)	1.9	0.64	1.9	0.64
	Load shedding (MW)	34.9	894.7	24.7	938.6
Previous approaches	nadir (Hz)	49.2	0.006	49.4	0.0002
	RoCoF (Hz/s)	0.6	0.005	0.5	0.0002
	Inertia change (s)	—	—	—	—
	Load shedding (MW)	—	—	—	—

homogeneous values when such aspects are not included in the simulations, with a typical deviation near zero. In addition, and according to the remarkable frequency excursion dependence on different parameters such as on power system rotational inertia, generation unit technologies and rate power of the tripping-generation unit; controller parameters should dynamically vary in line with those power system variables and at the same time keeping frequency requirements. These aspects are currently under analysis by the authors for further contributions. Whereas our findings are derived based on a single-islanding power system case study, our results are useful and significant based on the relevance of our realistic case study coupled with the number of different energy scenarios and wind power integration ranges.

6. Acknowledgment

Authors thank Ignacio Ares for the preliminary analyses that he did as part of his final master project.

7. Funding

This work has been partially supported the Spanish Ministry of Economy and Competitiveness under the project ‘Value of pumped-hydro energy storage in isolated power systems with high wind power penetration’ of the National Plan for Scientific and Technical Research and Innovation 2013-2016 (Ref. ENE2016-77951-R) and by the Spanish Education, Culture and Sports Ministry (Ref. FPU16/04282).

References

- [1] P. Tielens, D. Van Hertem, The relevance of inertia in power systems, *Renewable and Sustainable Energy Reviews* 55 (2016) 999–1009.
- [2] W. Zhang, K. Fang, Controlling active power of wind farms to participate in load frequency control of power systems, *IET Generation, Transmission & Distribution* 11 (9) (2017) 2194–2203.
- [3] A. Fernández-Guillamón, E. Gómez-Lázaro, E. Muljadi, Á. Molina-García, Power systems with high renewable energy sources: A review of inertia and frequency control strategies over time, *Renewable and Sustainable Energy Reviews* 115 (2019) 109369.
- [4] A. Junyent-Ferr, Y. Pipelzadeh, T. C. Green, Blending HVDC-link energy storage and offshore wind turbine inertia for fast frequency response, *IEEE Transactions on sustainable energy* 6 (3) (2015) 1059–1066.
- [5] P. Tian, X. Xiao, K. Wang, R. Ding, A hierarchical energy management system based on hierarchical optimization for microgrid community economic operation, *IEEE Transactions on Smart Grid* 7 (5) (2016) 2230–2241.
- [6] Z. Akhtar, B. Chaudhuri, S. Y. R. Hui, Primary frequency control contribution from smart loads using reactive compensation, *IEEE Transactions on Smart Grid* 6 (5) (2015) 2356–2365.
- [7] S. Yang, J. Fang, Y. Tang, H. Qiu, C. Dong, P. Wang, Synthetic-inertia-based modular multilevel converter frequency control for improved micro-grid frequency regulation, in: 2018 IEEE Energy Conversion Congress and Exposition (ECCE), IEEE, 2018, pp. 5177–5184.
- [8] A. Fernandez-Guillamon, A. Viguera-Rodriguez, A. Garcia, Analysis of power system inertia estimation in high wind power plant integration scenarios, *IET Renewable Power Generation*.
- [9] M. Albadi, E. El-Saadany, Overview of wind power intermittency impacts on power systems, *Electric power systems research* 80 (6) (2010) 627–632.
- [10] G. Martínez-Lucas, J. I. Sarasúa, J. Á. Sánchez-Fernández, Frequency regulation of a hybrid wind-hydro power plant in an isolated power system, *Energies* 11 (1) (2018) 239.
- [11] P. Breeze, Chapter 11 — wind power, in: P. Breeze (Ed.), *Power Generation Technologies (Second Edition)*, second edition Edition, Newnes, Boston, 2014, pp. 223 – 242. doi: 10.1016/B978-0-08-098330-1.00011-9.
- [12] M. Edrah, K. L. Lo, O. Anaya-Lara, Impacts of high penetration of DFIG wind turbines on rotor angle stability of power systems, *IEEE Transactions on Sustainable Energy* 6 (3) (2015) 759–766.
- [13] R. Syahputra, I. Soesanti, DFIG control scheme of wind power using anfis method in electrical power grid system.
- [14] E. Artigao, A. Honrubia-Escribano, E. Gomez-Lazaro, Current signature analysis to monitor DFIG wind turbine generators: A case study, *Renewable Energy* 116 (2018) 5–14.
- [15] C. Cardozo, W. van Ackooij, L. Capely, Cutting plane approaches for frequency constrained economic dispatch problems, *Electric Power Systems Research* 156 (2018) 54–63.
- [16] P. Li, Y. Liu, H. Xin, X. Jiang, A robust distributed economic dispatch strategy of virtual power plant under cyber-attacks, *IEEE Transactions on Industrial Informatics* 14 (10) (2018) 4343–4352.
- [17] M. Toulabi, S. Bahrami, A. M. Ranjbar, An input-to-state stability approach to inertial frequency response analysis of doubly-fed induction generator-based wind turbines, *IEEE Transactions on Energy Conversion* 32 (4) (2017) 1418–1431.
- [18] L. E. Sokoler, P. Vinter, R. Baerentsen, K. Edlund, J. B. Jorgensen, Contingency-constrained unit commitment in meshed isolated power systems, *IEEE Transactions on Power Systems* 31 (5) (2016) 3516–3526.
- [19] G. Zhang, E. Ela, Q. Wang, Market scheduling and pricing for primary and secondary frequency reserve, *IEEE Transactions on Power Systems*.
- [20] M. R. Khalghani, M. H. Khooban, E. Mahboubi-Moghaddam,

- N. Vafamand, M. Goodarzi, A self-tuning load frequency control strategy for microgrids: Human brain emotional learning, *International Journal of Electrical Power & Energy Systems* 75 (2016) 311–319.
- [21] M. Marzband, M. M. Moghaddam, M. F. Akorede, G. Khomeyrani, Adaptive load shedding scheme for frequency stability enhancement in microgrids, *Electric Power Systems Research* 140 (2016) 78–86.
- [22] B. Ozer, O. Arikan, G. Moral, A. Altintas, Extraction of primary and secondary frequency control from active power generation data of power plants, *International Journal of Electrical Power & Energy Systems* 73 (2015) 16–22.
- [23] M. R. Aghamohammadi, H. Abdolahinia, A new approach for optimal sizing of battery energy storage system for primary frequency control of islanded microgrid, *International Journal of Electrical Power & Energy Systems* 54 (2014) 325–333.
- [24] H. Jiang, J. Lin, Y. Song, D. J. Hill, MPC-based frequency control with demand-side participation: A case study in an isolated wind-aluminum power system, *IEEE Transactions on Power Systems* 30 (6) (2015) 3327–3337.
- [25] H. Jiang, J. Lin, Y. Song, S. You, Y. Zong, Explicit model predictive control applications in power systems: an agc study for an isolated industrial system, *IET Generation, Transmission & Distribution* 10 (4) (2016) 964–971.
- [26] ENTSO-E, Electricity balancing in Europe, https://docstore.entsoe.eu/Documents/Network%20codes%20documents/NC%20EB/entso-e_balancing_in%20_europe_report_Nov2018_web.pdf.
- [27] P.-K. Keung, P. Li, H. Banakar, B. T. Ooi, Kinetic energy of wind-turbine generators for system frequency support, *IEEE Transactions on Power Systems* 24 (1) (2009) 279–287.
- [28] S. El Itani, U. D. Annakkage, G. Joos, Short-term frequency support utilizing inertial response of dfig wind turbines, in: *Power and Energy Society General Meeting, 2011 IEEE*, IEEE, 2011, pp. 1–8.
- [29] T. Mahto, V. Mukherjee, A novel scaling factor based fuzzy logic controller for frequency control of an isolated hybrid power system, *Energy* 130 (2017) 339–350.
- [30] A. Abazari, M. G. Dozein, H. Monsef, An optimal fuzzy-logic based frequency control strategy in a high wind penetrated power system, *Journal of the Franklin Institute* 355 (14) (2018) 6262–6285.
- [31] A. Alsharafi, A. Besheer, H. Emara, Primary frequency response enhancement for future low inertia power systems using hybrid control technique, *Energies* 11 (4) (2018) 699.
- [32] H. Ma, B. Chowdhury, Working towards frequency regulation with wind plants: combined control approaches, *IET Renewable Power Generation* 4 (4) (2010) 308–316.
- [33] M. Wang-Hansen, R. Josefsson, H. Mehmedovic, Frequency controlling wind power modeling of control strategies, *IEEE transactions on sustainable energy* 4 (4) (2013) 954–959.
- [34] M. Kang, K. Kim, E. Muljadi, J.-W. Park, Y. C. Kang, Frequency control support of a doubly-fed induction generator based on the torque limit, *IEEE Transactions on Power Systems* 31 (6) (2016) 4575–4583.
- [35] D. Ochoa, S. Martinez, Frequency dependent strategy for mitigating wind power fluctuations of a doubly-fed induction generator wind turbine based on virtual inertia control and blade pitch angle regulation, *Renewable energy* 128 (2018) 108–124.
- [36] H. Bevrani, P. R. Daneshmand, Fuzzy logic-based load-frequency control concerning high penetration of wind turbines, *IEEE systems journal* 6 (1) (2011) 173–180.
- [37] S. Ma, H. Geng, G. Yang, B. C. Pal, Clustering-based coordinated control of large-scale wind farm for power system frequency support, *IEEE Transactions on Sustainable Energy* 9 (4) (2018) 1555–1564.
- [38] L. Badesa, F. Teng, G. Strbac, Simultaneous scheduling of multiple frequency services in stochastic unit commitment, *IEEE Transactions on Power Systems* 34 (5) (2019) 3858–3868. doi: 10.1109/TPWRS.2019.2905037.
- [39] Z.-S. Zhang, Y.-Z. Sun, J. Lin, G.-J. Li, Coordinated frequency regulation by doubly fed induction generator-based wind power plants, *IET Renewable Power Generation* 6 (1) (2012) 38–47.
- [40] Y. Mi, Y. Fu, D. Li, C. Wang, P. C. Loh, P. Wang, The sliding mode load frequency control for hybrid power system based on disturbance observer, *International Journal of Electrical Power & Energy Systems* 74 (2016) 446–452.
- [41] Y. Bao, J. Xu, S. Liao, Y. Sun, X. Li, Y. Jiang, D. Ke, J. Yang, X. Peng, Field verification of frequency control by energy-intensive loads for isolated power systems with high penetration of wind power, *IEEE Transactions on Power Systems* 33 (6) (2018) 6098–6108.
- [42] K. Chen, P. Peng, H. Li, T. Xu, C. Li, Dfig primary frequency regulation strategy with optimal dynamic droop control under variable wind speeds, in: *IOP Conference Series: Earth and Environmental Science*, Vol. 188, IOP Publishing, 2018, p. 012087.
- [43] F. Wilches-Bernal, J. H. Chow, J. J. Sanchez-Gasca, A fundamental study of applying wind turbines for power system frequency control, *IEEE Transactions on Power Systems* 31 (2) (2015) 1496–1505.
- [44] A. Aziz, A. T. Oo, A. Stojcevski, Analysis of frequency sensitive wind plant penetration effect on load frequency control of hybrid power system, *International Journal of Electrical Power & Energy Systems* 99 (2018) 603–617.
- [45] M. Farrokhabadi, C. A. Cañizares, K. Bhattacharya, Unit commitment for isolated microgrids considering frequency control, *IEEE Transactions on Smart Grid* 9 (4) (2018) 3270–3280.
- [46] F. Teng, V. Trovato, G. Strbac, Stochastic scheduling with inertia-dependent fast frequency response requirements, *IEEE Transactions on Power Systems* 31 (2) (2016) 1557–1566.
- [47] S. Padrón, M. Hernández, A. Falcón, Reducing under-frequency load shedding in isolated power systems using neural networks. gran canaria: a case study, *IEEE Transactions on Power Systems* 31 (1) (2015) 63–71.
- [48] J. P. Praene, M. H. Radanielina, V. R. Rakotoson, A. L. Andriamamonjy, F. Sinama, D. Morau, H. T. Rakotondramiarana, Electricity generation from renewables in madagascar: Opportunities and projections, *Renewable and Sustainable Energy Reviews* 76 (2017) 1066–1079.
- [49] METI, Japan’s energy plan, Tech. rep. (2015). URL https://www.enecho.meti.go.jp/en/category/brochures/pdf/energy_plan_2015.pdf
- [50] A. Zertek, G. Verbic, M. Pantos, A novel strategy for variable-speed wind turbines’ participation in primary frequency control, *IEEE Transactions on sustainable energy* 3 (4) (2012) 791–799.
- [51] M. H. Nazari, Z. Costello, M. J. Feizollahi, S. Grijalva, M. Egerstedt, Distributed frequency control of prosumer-based electric energy systems, *IEEE Transactions on Power Systems* 29 (6) (2014) 2934–2942.
- [52] M. R. V. Moghadam, R. T. Ma, R. Zhang, Distributed frequency control in smart grids via randomized demand response, *IEEE Transactions on Smart Grid* 5 (6) (2014) 2798–2809.
- [53] Y. Wang, H. Li, Y. Xu, Y. Tang, System frequency regulation in singapore using distributed energy storage systems, in: *2017 Asian Conference on Energy, Power and Transportation Electrification (ACEPT)*, IEEE, 2017, pp. 1–6.
- [54] C. Pradhan, C. N. Bhende, Online load frequency control in wind integrated power systems using modified jaya optimization, *Engineering Applications of Artificial Intelligence* 77 (2019) 212–228.
- [55] J. I. Sarasúa, G. Martínez-Lucas, M. Lafoz, Analysis of alternative frequency control schemes for increasing renewable energy penetration in el hierro island power system, *International Journal of Electrical Power & Energy Systems* 113 (2019) 807–823.
- [56] Red Eléctrica de España, n.d., Gran canaria — seguimiento de la demanda de energía eléctrica, <https://demanda.ree.es/visiona/canarias/gcanaria/>.
- [57] Ministerio de Industria, Energía y Turismo, Procedimientos de operación de los Sistemas eléctricos Insulares y Extrapeninsulares: P.O. 3.1; 3.2; 9; SEIE-1; SEIE-2.2; SEIE-2.3; SEIE-3.1; SEIE-7.1; SEIE-7.2; SEIE-8.2; SEIE-9, Boletín Oficial del Estado Edition (2012).

- [58] Ministerio de Industria Energía y Turismo, Real Decreto 738/2015, de 31 de julio, por el que se regula la actividad de producción de energía eléctrica y el procedimiento de despacho en los sistemas eléctricos de los territorios no peninsulares, Boletín Oficial del Estado Edition (2015).
- [59] D. Fernández-Muñoz, J. Pérez-Díaz, Contribution of non-conventional pumped-storage hydropower plant configurations in an isolated power system with an increasing share of renewable energy, *IET Renewable Power Generation* doi:10.1049/iet-rpg.2019.0874.
- [60] D. Fernández-Muñoz, J. I. Pérez-Díaz, M. Chazarra, A two-stage stochastic optimisation model for the water value calculation in a hybrid diesel/wind/pumped-storage power system, *IET Renewable Power Generation* 13 (12) (2019) 2156–2165.
- [61] R. Azizipanah-Abarghooee, F. Golestaneh, H. B. Gooi, J. Lin, F. Bavafa, V. Terzija, Corrective economic dispatch and operational cycles for probabilistic unit commitment with demand response and high wind power, *Applied Energy* 182 (2016) 634–651. doi:<https://doi.org/10.1016/j.apenergy.2016.07.117>.
- [62] M. Pezic, V. M. Cedrés, Unit commitment in fully renewable, hydro-wind energy systems, in: 2013 10th International Conference on the European Energy Market (EEM), IEEE, 2013, pp. 1–8.
- [63] G. Morales-España, J. M. Latorre, A. Ramos, Tight and compact milp formulation of start-up and shut-down ramping in unit commitment, *IEEE Transactions on Power Systems* 28 (2) (2013) 1288–1296.
- [64] S. Mansoor, D. Jones, D. A. Bradley, F. Aris, G. Jones, Reproducing oscillatory behaviour of a hydroelectric power station by computer simulation, *Control Engineering Practice* 8 (11) (2000) 1261–1272.
- [65] J. O’Sullivan, A. Rogers, D. Flynn, P. Smith, A. Mullane, M. O’Malley, Studying the maximum instantaneous non-synchronous generation in an island system—frequency stability challenges in ireland, *IEEE Transactions on Power Systems* 29 (6) (2014) 2943–2951.
- [66] P. Kundur, N. J. Balu, M. G. Lauby, *Power system stability and control*, Vol. 7, McGraw-hill New York, 1994.
- [67] NEPLAN AG, Turbine-governor models, standard dynamic turbine-governor systems, https://www.neplan.ch/wp-content/uploads/2015/08/Nep_TURBINES_GOV.pdf (2016).
- [68] J. I. Perez-Diaz, J. I. Sarasua, J. R. Wilhelmi, Contribution of a hydraulic short-circuit pumped-storage power plant to the load-frequency regulation of an isolated power system, *International Journal of Electrical Power & Energy Systems* 62 (2014) 199–211.
- [69] ENTSO-E, Continental Europe Operation Handbook, <https://docstore.entsoe.eu/publications/system-operations-reports/operation-handbook/Pages/default.aspx>.
- [70] A. J. Wood, B. F. Wollenberg, *Power generation, operation, and control*, John Wiley & Sons, 2012.
- [71] M. Pyller, S. Achilles, Aggregated wind park models for analyzing power system dynamics.
- [72] M. Mokhtari, F. Aminifar, Toward wide-area oscillation control through doubly-fed induction generator wind farms, *IEEE Transactions on Power Systems* 29 (6) (2014) 2985–2992.
- [73] L.-R. Chang-Chien, W.-T. Lin, Y.-C. Yin, Enhancing frequency response control by DFIGs in the high wind penetrated power systems, *IEEE transactions on power systems* 26 (2) (2010) 710–718.
- [74] I. Erlich, M. Wilch, Primary frequency control by wind turbines, in: IEEE PES general meeting, IEEE, 2010, pp. 1–8.
- [75] I. D. Margaritis, S. A. Papathanassiou, N. D. Hatziaargyriou, A. D. Hansen, P. Sorensen, Frequency control in autonomous power systems with high wind power penetration, *IEEE Transactions on Sustainable Energy* 3 (2) (2012) 189–199.
- [76] A. Žertek, G. Verbič, M. Pantoš, Optimised control approach for frequency-control contribution of variable speed wind turbines, *IET Renewable power generation* 6 (1) (2012) 17–23.
- [77] N. R. Ullah, T. Thiringer, D. Karlsson, Temporary primary frequency control support by variable speed wind turbines – potential and applications, *IEEE Transactions on Power Systems* 23 (2) (2008) 601–612.
- [78] K. Clark, N. W. Miller, J. J. Sanchez-Gasca, Modeling of GE wind turbine-generators for grid studies, *GE Energy* 4 (2010) 0885–8950.
- [79] A. Jafari, G. Shahgholian, Analysis and simulation of a sliding mode controller for mechanical part of a doubly-fed induction generator-based wind turbine, *IET Generation, Transmission & Distribution* 11 (10) (2017) 2677–2688.
- [80] J. Liu, Y. Gao, S. Geng, L. Wu, Nonlinear control of variable speed wind turbines via fuzzy techniques, *IEEE Access* 5 (2017) 27–34.
- [81] F. Huerta, R. L. Tello, M. Prodanovic, Real-time power-hardware-in-the-loop implementation of variable-speed wind turbines, *IEEE Transactions on Industrial Electronics* 64 (3) (2017) 1893–1904.
- [82] A. Fernández-Guillamón, J. Villena-Lapaz, A. Viguera-Rodríguez, T. García-Sánchez, Á. Molina-García, An adaptive frequency strategy for variable speed wind turbines: Application to high wind integration into power systems, *Energies* 11 (6) (2018) 1436.
- [83] A. Fernández-Guillamón, A. Viguera-Rodríguez, E. Gómez-Lázaro, Á. Molina-García, Fast power reserve emulation strategy for vswt supporting frequency control in multi-area power systems, *Energies* 11 (10) (2018) 2775.
- [84] G. C. Tarnowski, P. C. Kjar, P. E. Sorensen, J. Ostergaard, Variable speed wind turbines capability for temporary overproduction, in: Power & Energy Society General Meeting, 2009. PES’09. IEEE, IEEE, 2009, pp. 1–7.
- [85] G. Lalor, A. Mullane, M. O’Malley, Frequency control and wind turbine technologies, *IEEE Transactions on power systems* 20 (4) (2005) 1905–1913.
- [86] L. Sigrist, I. Egido, E. F. Sanchez-Ubeda, L. Rouco, Representative operating and contingency scenarios for the design of ufls schemes, *IEEE Transactions on Power Systems* 25 (2) (2009) 906–913.
- [87] P. Daly, D. Flynn, N. Cunniffe, Inertia considerations within unit commitment and economic dispatch for systems with high non-synchronous penetrations, in: PowerTech, 2015 IEEE Eindhoven, IEEE, 2015, pp. 1–6.